JOURNAL OF GEOPHYSICAL RESEARCH, VOL. 99, NO. C5, PAGES 10,275–10,287, MAY 15, 1994

# The distribution of $^{14}C$ and $^{39}Ar$ in the Weddell Sea

P. Schlosser,[1,2] B. Kromer,[3] R. Weppernig,[1,4] H.H. Loosli,[4] R. Bayer,[3]
G. Bonani,[5] and M. Suter [5]

**Abstract.** Carbon 14 and $^{39}Ar$ data from the Weddell Sea are presented and discussed. Values of $\Delta\,^{14}C$ and $^{39}Ar$ are low in the winter mixed layer ($\Delta\,^{14}C \approx -90$ to $-125$ ‰; $^{39}Ar \approx 85$ % modern). These low values are consistent with the surface layer dynamics which is dominated by entrainment of relatively old water of circumpolar origin and reduced gas exchange during sea ice cover. The $\Delta\,^{14}C$ and $^{39}Ar$ values of the deep and bottom waters range from $-160$ to $-150$ ‰ and 38 to 57 % modern, respectively. The $\Delta\,^{14}C$ values of Weddell Sea Bottom Water (WSBW) found in the central Weddell Sea along a 0° longitude section are only slightly higher than those of the overlying Weddell Sea Deep Water (WSDW) showing that the influence of bomb $^{14}C$ on these waters is small. Part of the WSBW with higher $\Delta\,^{14}C$ values observed in the northwestern Weddell Sea seems to escape through the South Sandwich Trench, and part seems to mix from a boundary current into the central Weddell Sea. The observed $^{14}C$ distribution is consistent with the hypothesis that Ice Shelf Water (ISW) is a source of WSBW. A simple conceptual model of the surface layer dynamics is used to estimate the prebomb $\Delta\,^{14}C$ values of Surface Water and Winter Water to be about $-140$ and $-130$ ‰, respectively. Using mixing ratios between WSDW and shelf water derived from temperature/salinity and $^{3}He$ data, the prebomb $\Delta\,^{14}C$ values of WSBW are estimated to be $-157$ ‰ (potential temperature of WSBW: $-0.7$ °C). The $^{39}Ar$ concentration of WSBW with a potential temperature of $-0.7$ °C is determined to be 57 % modern. Bomb radiocarbon water column inventories are estimated and discussed.

## Introduction

Measurement of the radioactive isotope of carbon, $^{14}C$, offers a tool to study the flow pattern and mean residence time of the deep and abyssal waters in the ocean [e.g., *Broecker et al.*, 1960, 1985; *Münnich and Roether*, 1967; *Stuiver et al.*, 1983]. In such studies the $^{14}C$ gradient between the deep water formation region and the deep basins, which is caused by radioactive decay, is converted into a mean "age" of the deep water [e.g., *Broecker et al.*, 1991]. During the past three decades, efforts have been made to map the global distribution of $^{14}C$ mainly in the framework of geochemical programs such as Geochemical Ocean Sections (GEOSECS), Transient Tracers in the Ocean (TTO) or the South Atlantic Ventilation Experiment (SAVE). These programs established a $^{14}C$ database on a course grid for most major basins of the world ocean. However, the regions of deep water formation in the Southern Ocean were not adequately sampled due to the special logistics required in ice-covered areas. In the Weddell Sea, which is regarded as a major source of Southern Ocean deep water, only a limited $^{14}C$ sampling program could be performed in the framework of the International Weddell Sea Oceanographic Expedition (IWSOE) in 1973, yielding $^{14}C$ data from the near-surface waters on a section across the Weddell Sea along the Greenwich meridian and from stations on the southern shelves in the vicinity of the Filchner Depression [*Weiss et al.*, 1979]. To fill the gap of $^{14}C$ data in the Weddell Sea, we collected samples on three cruises of the German research icebreaker *Polarstern* to the Weddell Sea on stations covering the entire water column with good depth resolution. The main objective was to obtain a data set allowing an estimate of the prebomb $^{14}C$ concentrations of the Weddell Sea surface and deep waters.

The application of $^{14}C$ is complicated by the fact that so-called bomb $^{14}C$ delivered to the atmosphere during the surface nuclear weapon tests mainly in the mid-1960s enters the surface water of the oceans in the form of $^{14}CO_2$ and masks the natural $^{14}C$ distribution. Because relatively few $^{14}C$ data exist from the prebomb era, it is difficult to determine the natural $^{14}C$ distribution in the ocean surface waters accurately. These

[1] Lamont–Doherty Earth Observatory, Palisades, New York
[2] Department of Geological Sciences, Columbia University, New York
[3] Institut für Umweltphysik der Universität Heidelberg, Germany
[4] Physikalisches Institut der Universität Bern, Switzerland
[5] Institut für Mittelenergiephysik, ETH Zürich, Switzerland



Paper number 94JC00313.
0148-0227/94/94JC-00313$05.00

uncertainties in the initial $\Delta\,^{14}C$ values might influence the estimates of the deep water renewal times derived from measured $^{14}C$ distributions. The noble gas isotope $^{39}Ar$ with a half life of 269 years has a much simpler boundary condition and is therefore principally better suited to determine the timescale of the deep water circulation. Present techniques for measurement of $^{39}Ar$ require large amounts of water and long counting times in special ultra low-level laboratories [*Loosli*, 1983], restricting sampling to the major water masses of the world ocean without significant spatial resolution. However, these data should be sufficient to "calibrate" the $^{14}C$ measurements which can be obtained on a denser grid, allowing resolution of the fine structures. For this reason, we sampled the main water masses in the Weddell Sea for $^{39}Ar$ in the framework of our $^{14}C$ program to establish the $^{39}Ar$ concentration of deep and bottom waters formed in the Weddell Sea.

The purpose of this contribution is to present our $^{14}C$ and $^{39}Ar$ data and to estimate the initial $\Delta\,^{14}C$ values and $^{39}Ar$ concentrations in Weddell Sea deep and bottom water.

## Sample Collection and Measurement

The $^{14}C$ data set discussed here was collected on legs 2, 3, and 4 of the fifth cruise of *Polarstern* to the Weddell Sea (ANT V). The major part of the data was collected during ANT V/2 (Winter Weddell Sea Experiment; June to September 1986) on a section across the Weddell Gyre at about 0° longitude (Figure 1) using large-volume samplers for high precision measurement by low-level counting. Additional samples were taken on the southern and southwestern shelves and in the bottom water of the northwestern Weddell Sea during ANT V/3 (September to December 1986) and ANT V/4 (January to March 1987; Figure 1). The ANT V/3 data were obtained by both low-level counting technique and accelerator mass spectrometry (AMS); on ANT V/4 only samples for AMS $^{14}C$ measurements were taken. Argon 39 samples were collected mainly during ANT V/2 with some additional sampling on ANT V/3.

Sampling and measurement procedures for large- and small-volume $^{14}C$ have been described by *Schlosser et al.* [1989]. The data are reported as age corrected $\Delta\,^{14}C$, following *Stuiver and Polach* [1977]. The overall error of the $\Delta\,^{14}C$ values is ±2‰. The data refer to the 1983 recalibration of the Heidelberg sodium carbonate substandard to National Bureau of Standards (NBS) oxalic acid [*Kromer*, 1984]. The small-volume $^{14}C$ samples were measured at the Zürich AMS facility after $CO_2$ extraction and target preparation at Heidelberg. The precision of the AMS $^{14}C$ data is about ±5 to 6‰. Details of the procedure are described by *Kromer et al.* [1987].

At some stations the gases extracted from five Gerard samplers (wire length between the samplers was 15 m) were collected in stainless steel cylinders for $^{39}Ar$ measurement. Argon 39 measurements were performed at Bern using low-level counting techniques in an underground laboratory. Ar and Kr fractions were separated by gas chromatography followed by purification. The extraction and separation yield was checked by comparison of the amount of the extracted gases with that expected from the amount of water and the argon sol-

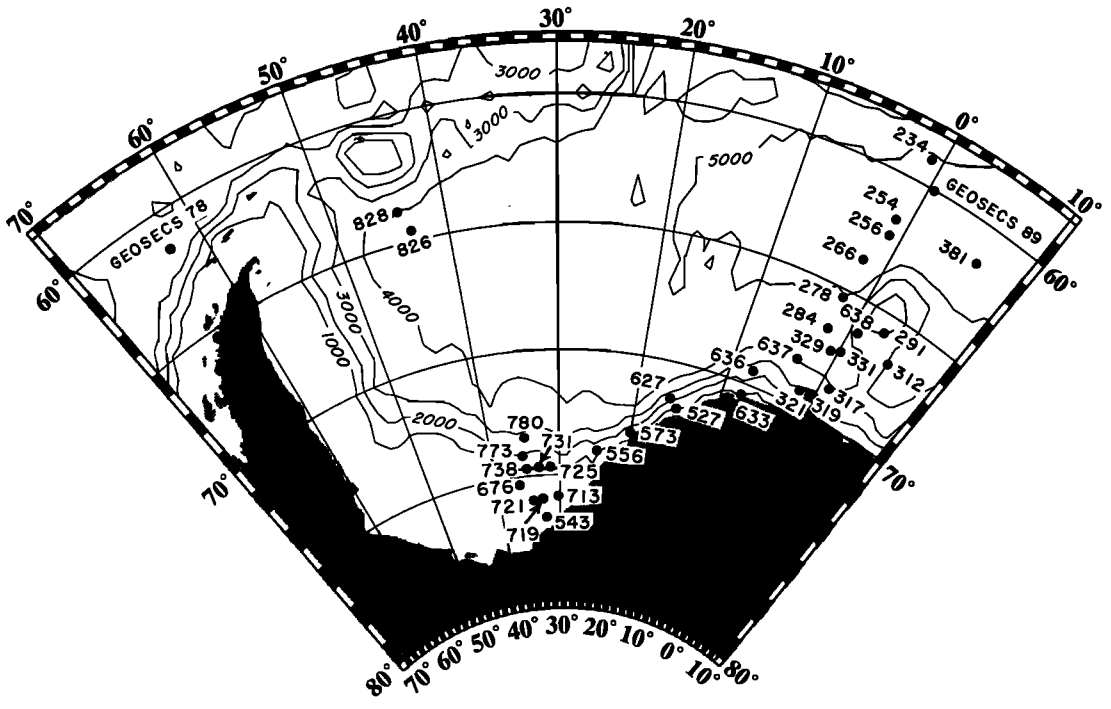


**Figure 1.** Geographical positions of the stations occupied during WWSP 86 and ANT V/4 (stations 773, 780, 826, 828).

ubility in water. Additionally, $^{85}Kr$ was measured on each $^{39}Ar$ sample as an indicator of contamination with air. The $^{39}Ar$ data are reported in "units" of "% modern". This notation means the activity of the sample expressed as percent fraction of an atmospheric air standard taken in 1983 and decay corrected to the time of measurement. The $^{39}Ar$ data are then decay corrected to the date of sampling. The precision of the data is about ±4 to 5% . Details of the procedures are described by *Loosli* [1983].

## Hydrographic Background

To provide background for the discussion of the $^{14}C$ and $^{39}Ar$ data the hydrography of the Weddell Sea is briefly summarized in this section. The main hydrographic features of the central Weddell Sea are shown using the temperature/salinity data from the ANTV $^{14}C$ stations (Figure 2 and Plate 1; for position of the stations, see Figure 1). Water from the Antarctic Circumpolar Current (ACC) is flowing into the Weddell Sea and can be recognized as a distinct temperature and salinity maximum at intermediate depths (several hundred meters; Figure 2 and Plate 1). We call the waters with potential temperatures above 0.2° Circumpolar Deep Water (CDW) because this water originates from the deep water horizons found in the Drake Passage [*Sievers and Nowlin*, 1984; *Whitworth and Nowlin*, 1987]. The CDW is separated by a weak pycnocline from the surface waters. In winter, a layer of about 100-m thickness with temperatures close to the freezing point is formed under the sea ice cover [*Gordon and Huber*, 1984, 1990]. After the sea ice cover retreats in summer, the surface water is diluted by melt water and warmed up to several degrees Celsius (Antarctic Surface Water; ASW), while at about 80- to 100-m depth the remnant of the winter mixed layer marked by a distinct

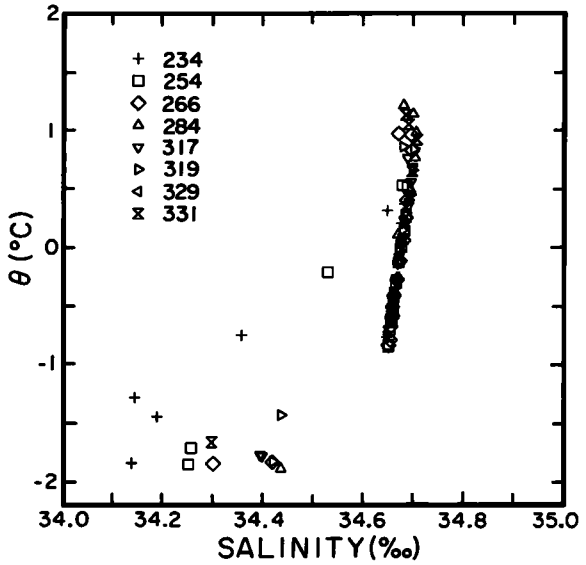


**Figure 2.** Potential temperature versus salinity plot for the same stations as in Plate 1. Salinity samples were drawn from the Gerard–Ewing samplers.

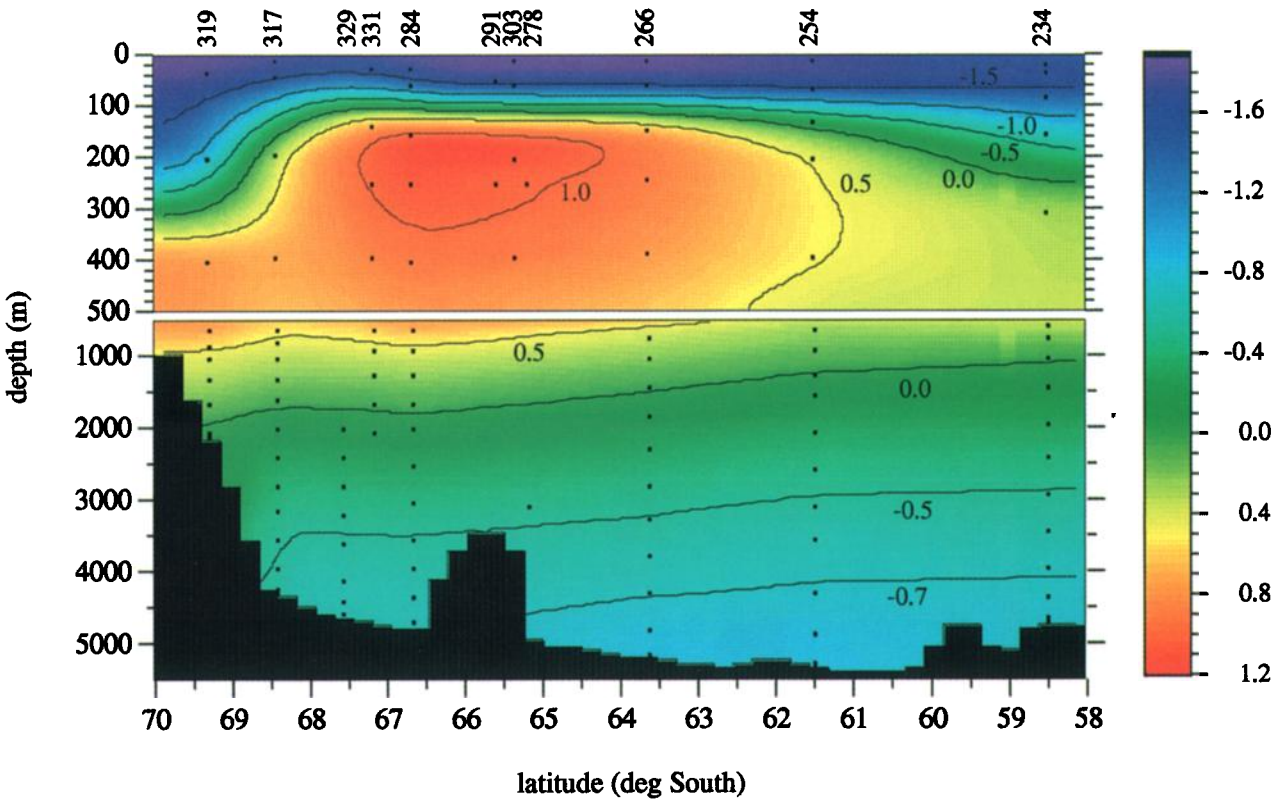


**Plate 1.** Potential temperature section along the 0° longitude section (data from reversing thermometers attached to the Gerard–Ewing water samplers).

temperature minimum with values close to the freezing point is preserved (Winter Water; WW). The temperature of the waters below CDW decreases steadily with depth to values below −0.7 °C near the bottom. Following *Carmack and Foster* [1975a] the water with potential temperatures below −0.7 °C is called Weddell Sea Bottom Water (WSBW). The water between the WSBW and the CDW is called Weddell Sea Deep Water (WSDW).

The shelf waters found in the Weddell Sea are usually divided into Eastern Shelf Water (ESW), Western Shelf Water (WSW) and Ice Shelf Water (ISW) [e.g. *Carmack and Foster*, 1975b]. ESW with potential temperatures between −1.6 and −2.0 °C and salinities between 34.28 and 34.44 is found on the shelves east of the Filchner Depression. WSW has the same potential temperature range but higher salinities than ESW (34.56 to 34.84) and occupies the shelf region west of the Filchner Depression. ISW is characterized by potential temperatures below the freezing point of seawater at surface pressure and salinities of 34.56 to 34.68. It is formed by modification of WSW due to interaction with glacial ice under the Filchner/Ronne ice shelf [*Foldvik et al.*, 1985a,b].

Deep and bottom water formation in the Weddell Sea is still not well understood. Waters with potential temperatures below about 0.2 °C cannot be derived directly from the ACC [*Whitworth and Nowlin*, 1987] but instead have to be formed in the Weddell Sea or advected from other areas such as the Scotia Sea. It is evident from analysis of the distributions of temperature/salinity and other tracers that the deep and bottom waters are made up of a mixture between cold and ventilated shelf waters and CDW. There are different hypotheses about the processes leading to WSBW formation, such as the overflow of ISW followed by subsequent entrainment of WSDW [*Foldvik et al.*, 1985a,b,c] or the mixing of modified CDW with WW and WSW [*Foster and Carmack*, 1976]. Although direct observations of the overflow process provide evidence for the contribution of ISW to WSBW [*Foldvik et al.*, 1985a,b,c; *Schlosser et al.*, 1990], it is still an open question which other processes contribute to deep and bottom water formation. Breaks and nonlinearities in potential temperature/salinity [*Carmack and Foster*, 1975a] and other tracer characteristics of waters lying between CDW and WSBW point toward a complex pattern of mixing within, and perhaps advection of, waters into the Weddell Sea, leading finally to the Weddell Sea deep and bottom waters. It seems likely that different processes contribute to deep and bottom waters found in different depth intervals. Both the density and the rate of deep water produced by the individual processes are most likely highly variable in space and time.

## Observed $^{14}C$ and $^{39}Ar$ Distributions

### Carbon 14

The main features of the $^{14}C$ distribution at stations in the central Weddell Sea have been described before [*Schlosser et al.*, 1987, 1989] and are only briefly summarized. The $^{14}C$ distribution along the ANT V/2 section (stations 234, 254, 266, 284, 317, 319, 329 and

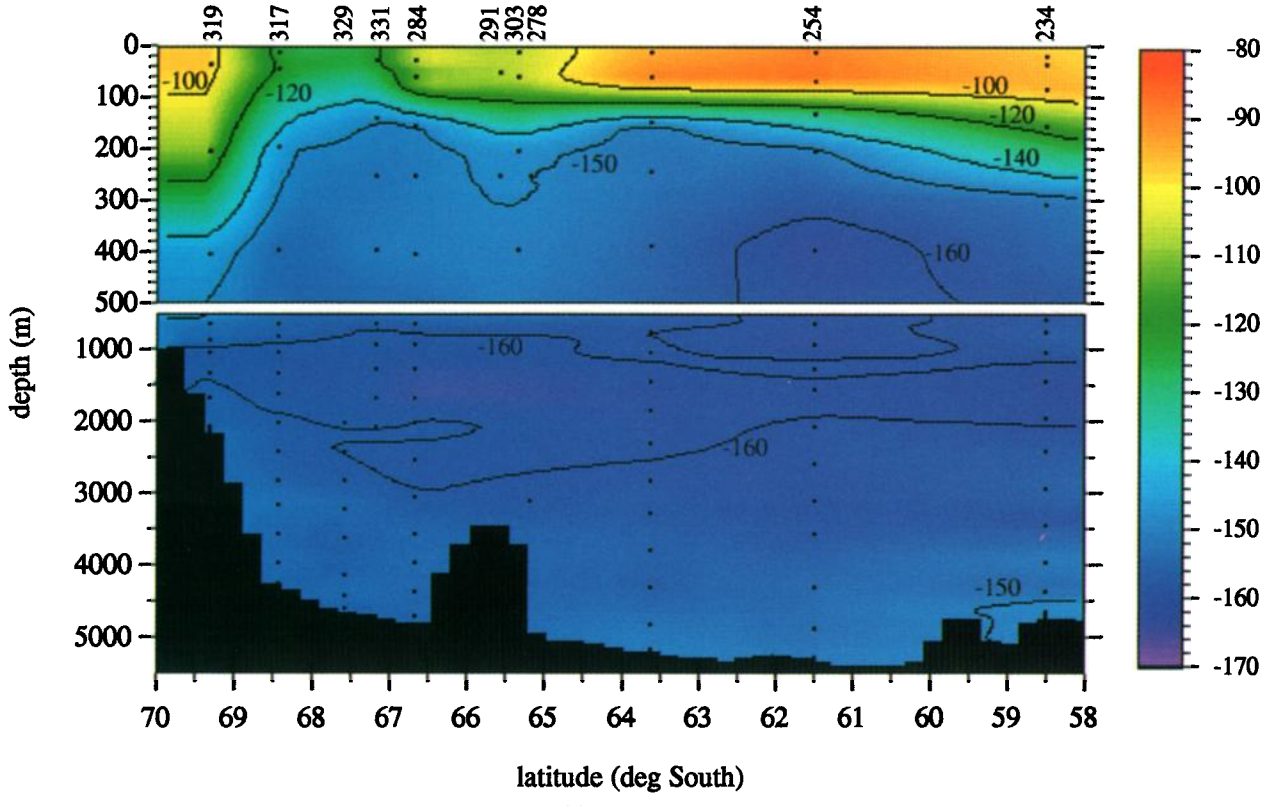


**Plate 2.** The $\Delta^{14}C$ section along 0° longitude.

331; Figure 1) is characterized by surface $\Delta^{14}C$ values between about −85‰ and −125‰ (Plate 2). Below the winter mixed layer, which at most stations is about 100 m thick (average of the ANT V/2 stations is 111 m [*Gordon and Huber*, 1990]), $\Delta^{14}C$ values drop below −150‰ and reach a minimum at a depth of about 1500 to 2000 m with $\Delta^{14}C$ values between about −160 and −165‰ (Plate 2). Towards the bottom, the $\Delta^{14}C$ values increase monotonically to values ranging from −149‰ at stations 234 and 254 (northern Weddell Sea) to about −157‰ in the southern Weddell Sea (Plate 2). Station 319 located on the continental slope of the southern Weddell Sea (Figure 1) shows slightly higher $\Delta^{14}C$ values (of the order of 5‰) at almost all depths below the surface surface layer.

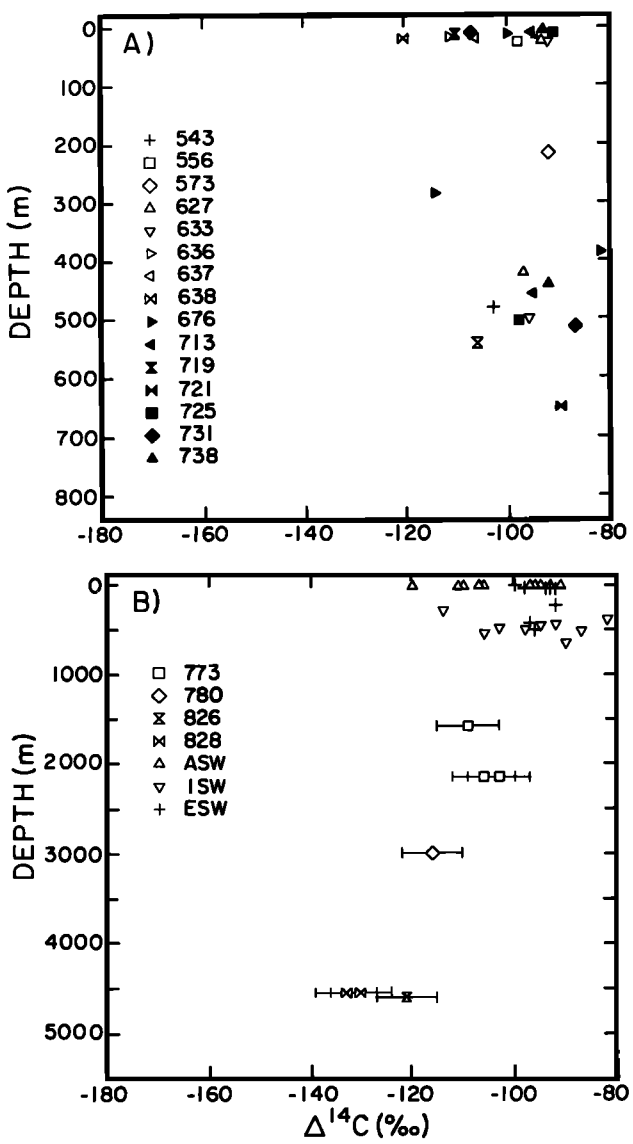


**Figure 3.** (a) Depth profiles of $\Delta^{14}C$ for stations located on the shelf (for geographic position, see Figure 1). (b) Same as Figure 3a for stations located on the continental slope (stations 773, 780, 826, 828). The $\Delta^{14}C$ values of the shelf samples are categorized by water mass.

Carbon 14 varies in shelf waters within a wide range (Figure 3a). ESW has relatively uniform $^{14}C$ concentrations of about −92 to −100‰ (Figure 3b). $\Delta^{14}C$ values of ISW cover the range between −82 and −114‰ with most data points falling in the interval between −90 and −105‰ (Figure 3b). Most of the shelf stations have surface $\Delta^{14}C$ values between −90 and −110 ‰ (Figure 3b). The few samples collected on the continental slope in the southern Weddell Sea north of the Filchner Depression (stations 773 and 780) show $\Delta^{14}C$ values between −103 and −116‰ (Fig. 4b). These samples were collected from the bottom layer, which consists of a mixture of ISW overflowing the sill that separates the Filchner Depression from the Weddell Sea and WSDW. The $^{14}C$ concentration of the WSBW collected at stations 826 and 828 in the northwestern Weddell Sea is between −121 and −133‰ (Figure 3b).

### Argon 39

The $^{39}Ar$ concentrations of the surface waters sampled during ANT V/2/3 reach from about 84% modern in the ice-covered central Weddell Sea (Figure 4) to about 95% modern in the shelf waters. The values in CDW range between 37 and 46% modern (Figure 4). Below the CDW the $^{39}Ar$ concentrations are between 34 and 52% modern in WSDW and increase to 52 to 57% modern in WSBW (Figure 4). The $^{39}Ar$ data are summarized in the form of a depth profile in Figure 5. The $^{39}Ar$ concentrations observed in shelf waters (ESW and ISW) during ANT V/3 are about 95% modern and are included in Figure 5.

## Discussion

### Surface Waters

The Weddell Sea surface waters (ASW and WW) have exceptionally low $\Delta^{14}C$ values compared to surface waters of lower latitudes. The reason for this feature is suppressed exchange of $CO_2$ with the atmosphere due to ice cover in winter and upwelling of "old" water originating from the circumpolar flow regime into the winter mixed layer of the Weddell Sea [*Schlosser et al.*, 1989]. The incorporation of CDW into the winter mixed layer is driven by convection induced by brine release during sea ice formation. Our data collected during ANT V/2 show $\Delta^{14}C$ values decreasing from about −90‰ in the northern Weddell Sea to −125‰ in the southern Weddell Sea (Figure 6). These values can be checked for consistency with the water balance of the winter mixed layer obtained from the analysis of oxygen data [*Gordon and Huber*, 1990]. For this purpose the $\Delta^{14}C$ values of the mixed layer at the time when the ice cover started to suppress gas exchange with the atmosphere has to be known. As no direct measurements are available, we have to estimate this value from the surface $^{14}C$ data obtained on stations 234 and 254, which only to a minor extent should have been affected by upwelling of CDW at the time of sampling. The $\Delta^{14}C$ values of the surface water at these

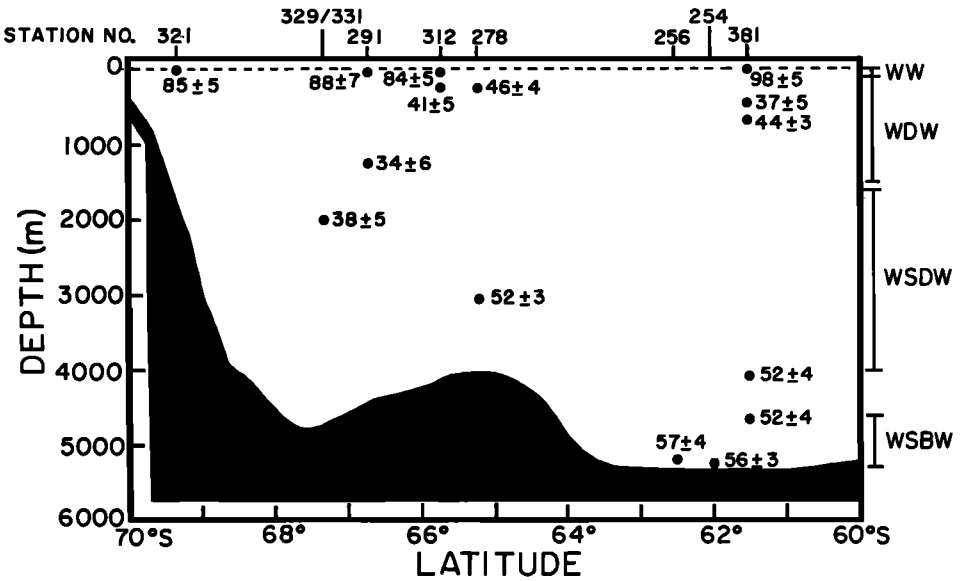


**Figure 4.** The $^{39}$Ar results plotted on a section across the Weddell Sea along 0° longitude.

stations are −96 and −88 ‰ (Figure 6). Summer data from a station occupied during ANT III (January to March 1985) yield similar values (−89 ‰ [*Schlosser et al.*, 1987]). Assuming that the summer values at the time of sampling in January had not yet reached their maximum, we set the initial $^{14}$C of the winter mixed layer to −85 ‰. Carbon 14 of the water underlying the winter mixed layer is about −153 ‰ (see below). Using the average entrainment rate of CDW into the winter mixed layer of 45 m y$^{-1}$ derived by *Gordon and Huber* [1990] and their mean thickness of the winter mixed layer of 111 m, we can calculate the expected average $\Delta^{14}$C values of the winter mixed layer to be −105 ‰. This value is in good agreement with the observations, which yield an average $\Delta^{14}$C value of −107 ‰ (station 319 which is influenced by the coastal current was not used in the calculation of the average $\Delta^{14}$C values). In the above calculations we did not correct for the different total inorganic carbon (TIC) concentrations of the different water masses because such a correction is only of the order of some percent. This simple balance shows that the $^{14}$C pattern observed in the Weddell Sea surface waters is consistent with the surface layer dynamics.

Argon 39 concentrations of the winter mixed layer at stations 291 and 321 are about 85 % modern. The difference of about 15 % between this observation and the $^{39}$Ar concentration of a sample equilibrated with the atmosphere (by definition 100 % modern) is consistent with the mixed layer balance discussed in the previous section. The average $^{39}$Ar concentration of the shelf

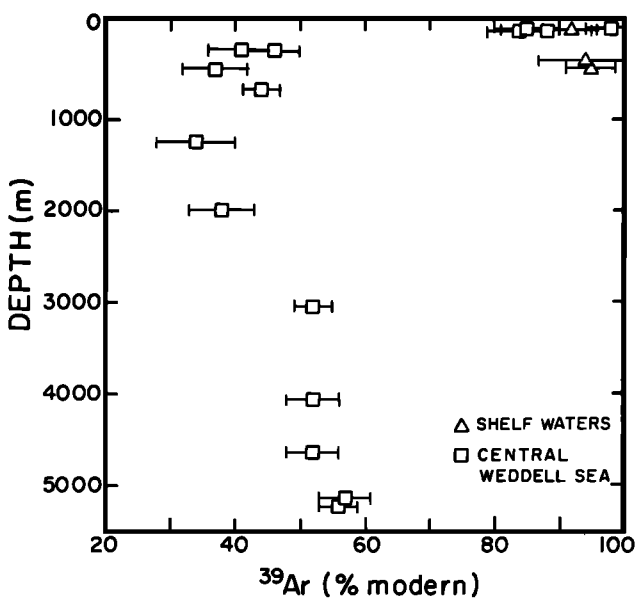


**Figure 5.** The $^{39}$Ar data summarized in a composite depth profile.

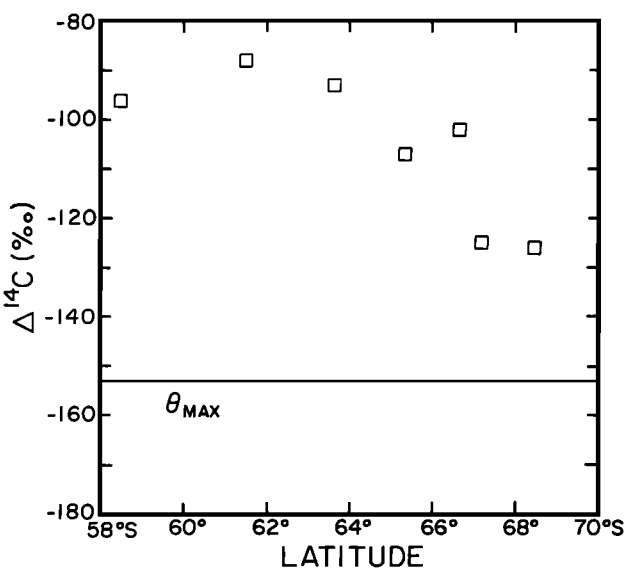


**Figure 6.** The $\Delta^{14}$C values in the winter mixed layer as a function of latitude along the 0° longitude section.

waters sampled during ANT V/3 (stations 527, 543 and 627) is (94±3) % modern, significantly below the solubility equilibrium with the atmosphere. This feature is consistent with the $\Delta\,^{14}C$ observed in shelf water, which are lower than the summer surface values in the central Weddell Sea. The reason for the relatively low $^{39}Ar$ and $^{14}C$ concentrations in the shelf waters which are derived from circumpolar water is incomplete equilibration with the atmosphere.

### Deep and Bottom Waters

The $^{14}C$ distribution in the water layers below ASW and WW are laterally relatively homogeneous. There are no significant deviations in $\Delta\,^{14}C$ from the mean value of −153 ‰ in the temperature maximum layer along the ANT V/2 section (Figure 7). The same holds true for the $\Theta$=0 °C isotherm with a mean $\Delta\,^{14}C$ value of −161 ‰. There is a slight increase of about 8 ‰ in $\Delta\,^{14}C$ in the deep and bottom water from the southern to the northern end of the section (Figure 7). This increase is related to the fact that at stations from the northern part of the section (stations 234, 254, 256, and 266), which are closer to the source of WSBW, the bottom layer consists of colder and fresher water ($\Theta \leq -0.7$ °C). In the southern part of the section (stations 284, 317, and 329), the bottom water has potential temperatures above −0.7 °C, indicating dilution by older water. Additionally, the bottom water found at the northern end of the ANT V/2 section is influenced to a larger degree by bomb $^{14}C$ than that observed in the southern part. This feature is evident from the distribution of tritium in the bottom waters of the Weddell Sea (Figure 8; see also *Bayer and Schlosser* [1991] and *Schlosser et al.* [1991]).

The deep waters found on the continental slope north of the Filchner Depression (stations 773 and 780) and in the northwestern corner of the Weddell Sea (stations 826 and 828) show $\Delta\,^{14}C$ values covering the range between the bottom waters at about 0° longitude and the surface waters of the shelf areas (Figure 3 b). There is a clear trend of decreasing $\Delta\,^{14}C$ with depth at these stations. This pattern is caused by increasing entrainment of deep waters with low $\Delta\,^{14}C$ values into the shelf water component flowing down the continental slope. In this

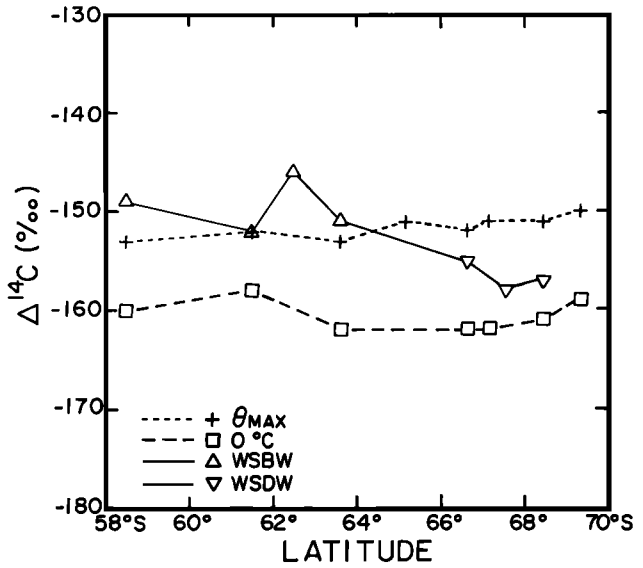


**Figure 7.** The $\Delta\,^{14}C$ values for three depth levels along the 0° longitude section. Different symbols for the bottom water values (deepest sample typically 10 to 20 m above ground) reflect the differnt water masses found at the bottom in the northern and southern parts of the section.

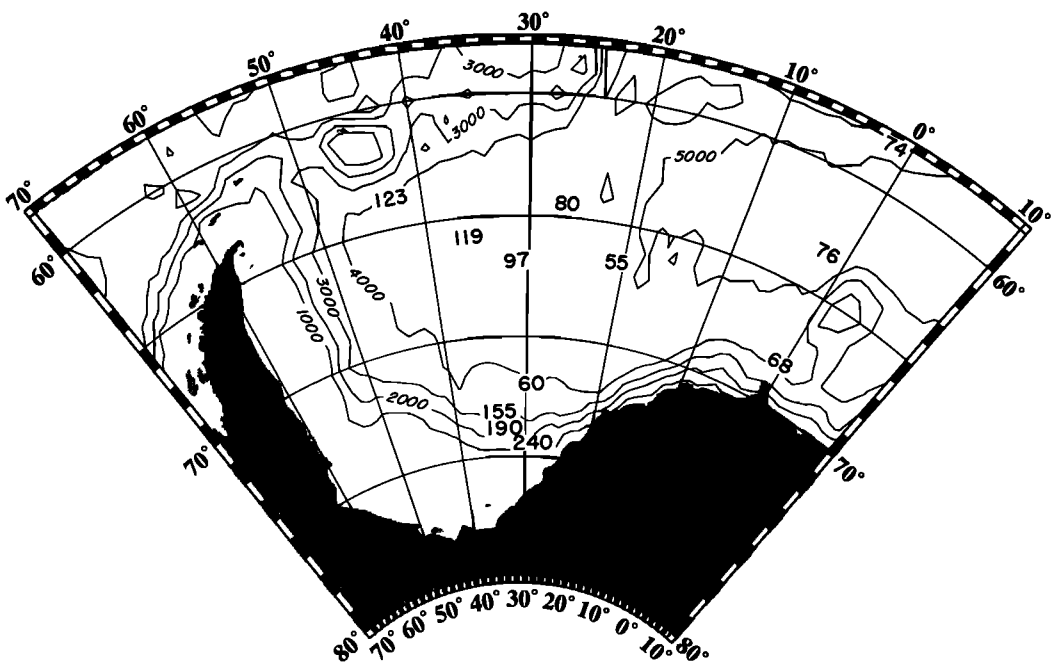


**Figure 8.** Bottom water tritium concentrations measured at different locations in the Weddell Sea (adapted from *Schlosser et al.* [1991]).

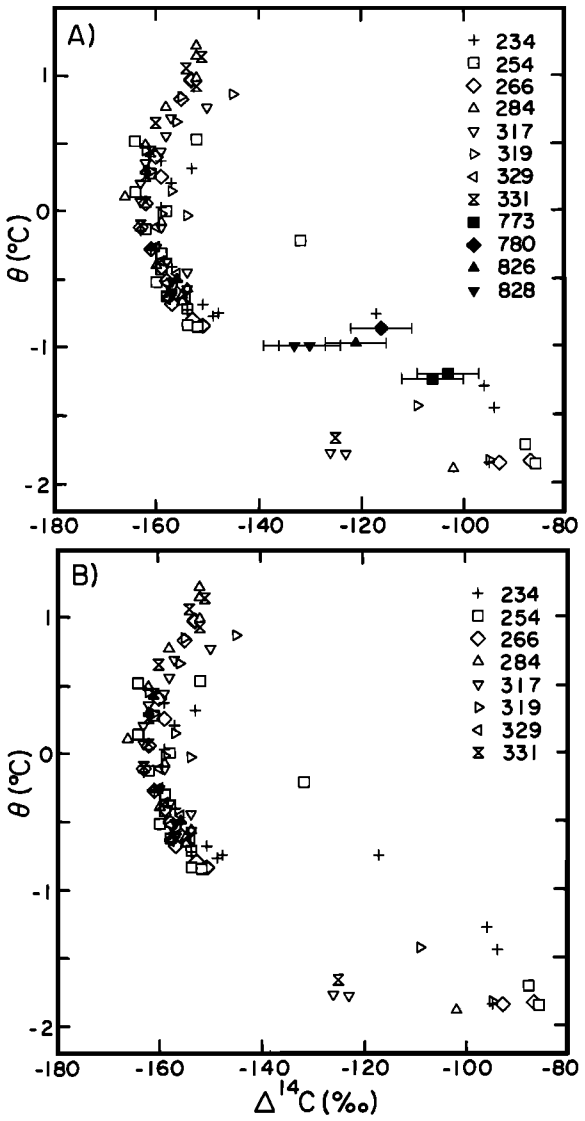


**Figure 9.** Potential temperature versus $\Delta\,^{14}C$ plot for (a) stations along the 0° longitude section and the continetal slope stations, and (b) the stations along the 0° longitude section only.

process, the entrained deep water component originates from successively larger depths.

To understand the distribution of $^{14}C$ in the Weddell Sea in terms of mixing of different water masses, the $\Delta\,^{14}C$ values are plotted versus potential temperature in Figure 9. There is a mixing regime between surface water with temperatures close to the freezing point and CDW which only is resolved at stations 234 and 254 (northern Weddell Sea) due to the sharp transition between the winter mixed layer and the underlying CDW at most of the ANT V stations (Figure 9 b). Below the pycnocline there seem to be two mixing regimes, one between the temperature maximum and water with a potential temperature of about 0 °C and one between the 0 °C layer and the bottom water. The overflowing water observed on the continental slope and the bottom waters in the northwestern corner of the Weddell Sea (stations 826 and 828) are a mixture of shelf water and water found at intermediate depths. The bottom water closer to the source region seems to mix with water from shallower layers, while subsequent entrainment of water to the overflowing shelf water is fed from deeper horizons. The scatter in the $\Delta\,^{14}C$ values of the bottom waters may at least in part be due to the relatively high variability of $^{14}C$ in ISW. The $^{14}C$ data are consistent with the hypothesis that ISW contributes to WSBW as suggested by hydrographic [*Foldvik et al.*, 1985a,b,c] and tracer data [*Weiss et al.*, 1979; *Schlosser et al.*, 1990].

The $\Delta\,^{14}C$ values observed in the bottom layer on the continental slope (stations 773 and 780) and in the northwestern Weddell Sea (stations 826 and 828) are relatively high compared to those found along 0° longitude. The reason for this feature is that the newly formed WSBW flows in a relatively narrow boundary current to the east, where part of it escapes to the north through the South Sandwich Fracture Zone at about 25 °W. The bottom water of the central Weddell Sea is renewed by mixing from this boundary current, part of which extends around the Weddell Gyre to the southern margin of the Weddell Sea. This pattern implies that the bottom water of the central Weddell Sea is less influenced by bomb $^{14}C$ contained in the shelf water than the newly formed WSBW observed at stations 826 and 828.

The $^{14}C$ versus potential temperature plot (Figure 9 b) suggests that WSBW is a mixture of cold shelf water and WSDW with a temperature of $\leq$0 °C. This feature is consistent with the hypothesis of *Foldvik and Gammelsød* [1988] that entrainment of WSDW into overflowing ISW occurs mainly at depths below about 2000 m. The basis for their conclusion is the observation of almost unmodified ISW on the continental slope northwest of the Filchner Depression at depths between

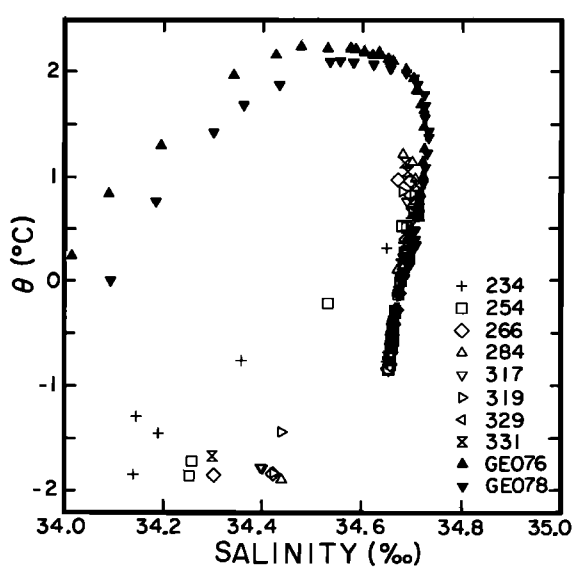


**Figure 10.** Potential temperature versus salinity plot of stations along the 0° longitude section in comparison to two GEOSECS stations located in the Drake Passage (stations GEO 76 and GEO 78).

1800 and 2000 m (see also *Schlosser et al.* [1990]). Further support for the above assumption is provided by the comparison of potential temperature/salinity data from Drake Passage and the Weddell Sea (Figure 10). Lower CDW found near the bottom in Drake Passage has almost exactly the same characteristics as the waters found in the Weddell Sea near the 0° isotherm. We interpret this feature as an indication that WSDW with potential temperatures close to 0 °C is basically undiluted lower CDW advected into the Weddell Sea. This water is entrained into the shelf water component during formation of WSBW on the continental slope north of the Filchner Depression.

The water above the 0 °C isotherm seems to be a mixture of CDW slightly influenced by bomb $^{14}C$, which is advected from the ACC into the Weddell Sea and WSDW with temperatures close to 0 °C. WSDW contains only a minor bomb $^{14}C$ component leading to a $^{14}C$ minimum in both the $^{14}C$ versus depth and the $^{14}C$ versus potential temperature plots (Plate 2 and Figure 9). Such a pattern of the $^{14}C$ distribution can be expected from the fact that bomb $^{14}C$ is transported to the bottom layers rapidly during WSBW formation, from where it mixes upward. At the same time, bomb $^{14}C$ enters the shallow water column by addition of shelf water to CDW and subsequent downward mixing. Even without a bomb component, the same pattern would evolve (although less pronounced) because the surface waters of the Weddell Sea are always higher in $^{14}C$ than CDW due to $CO_2$ exchange with the atmosphere.

The $^{39}Ar$ versus potential temperature plot (Figure 11) reflects the same basic feature as the $^{14}C/\Theta$ plot (Figure 9). The $^{39}Ar/\Theta$ plot is consistent with a linear mixing regime between water with a potential temperature of about 0 °C ($^{39}Ar \approx 35\%$ modern) and shelf waters with potential temperatures close to the freezing point and $^{39}Ar$ concentrations of about 95% modern. The water between the 0 °C isotherm and the temperature maximum shows a trend towards higher $^{39}Ar$ concentrations ($\approx 45\%$ modern), which is consistent with the assumption that the CDW contains a certain fraction of recently ventilated near-surface water. The only other alternative interpretation of the $^{39}Ar/\Theta$ plot would be the assumption that WSBW is a mixture between CDW and shelf water and the curvature of the observed $^{39}Ar/\Theta$ correlation is caused by the radioactive decay of $^{39}Ar$. This would lead to a mean renewal time of the intermediate waters in the Weddell Sea of the order of 125 years, which seems to be too long in view of its tritium concentrations (about 20% of the surface concentration observed in 1986).

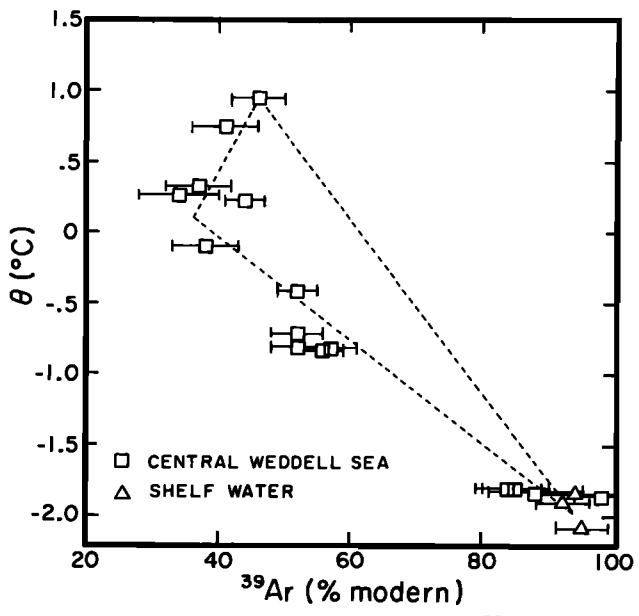


**Figure 11.** Potential temperature versus $^{39}Ar$ plot for all WWSP 86 samples.

The $^{39}Ar$ concentrations of Antarctic Bottom Water (AABW) and CDW have been estimated before on the basis of an extrapolation of the $^{14}C/^{39}Ar$ relationship of deep water from the equatorial and northeastern Atlantic to the southern source contributing to these waters [*Schlitzer et al.*, 1985]. The values obtained by this method (60± 7% modern for AABW and about 35% modern for Warm Deep Water in the Weddell Sea) are close to our measurements of about 52–57 and 42% modern, respectively.

## Prebomb $^{14}C$ in the Weddell Sea

Under certain favorable circumstances, bomb $^{14}C$ can be separated from the measured $\Delta^{14}C$ values using tritium/$^{14}C$ correlations. However, the tritium/$^{14}C$ ratio is variable in time and space and, generally, it is difficult to establish the proper ratio for areas with a complex hydrographic structure. We therefore chose a different way to estimate the prebomb $\Delta^{14}C$ values for the waters of the Weddell Sea: we simulate the $\Delta^{14}C$ values of surface water and WW as a function of time (starting at a time well before the bombtests) using a simple conceptual model of the mixed layer dynamics and the (measured) time-dependent atmospheric $^{14}C$ concentration. We then estimate the fraction of bomb $^{14}C$ in WSDW. As the bomb component in this water mass is very small, we can use the tritium/$^{14}C$ ratio to obtain a reasonable estimate. The prebomb $^{14}C$ concentrations of surface water and WSDW can then be used to estimate the prebomb $\Delta^{14}C$ value of WSBW based on the mixing considerations discussed above.

**Surface Waters** To simulate the $\Delta^{14}C$ value of surface water as a function of time, we follow the procedure described by *Schlosser et al.* [1989]. We assume that the winter mixed layer has an average thickness of 111 m [*Gordon and Huber*, 1990]. During winter, convection induced by brine release due to sea ice formation leads to entrainment of a 45-m-thick layer of CDW (Figure 12) with a $\Delta^{14}C$ value of about −153‰ (Figure 7). The −153‰ are estimated from our own data presented above (temperature maximum layer in Figure 7) and the data published by *Weiss et al.* [1979]. It might be a little too high due to a small bomb component in the upper CDW. However, the uncertainties introduced by the other parameters used in the model (entrainment rate of deep water into the surface

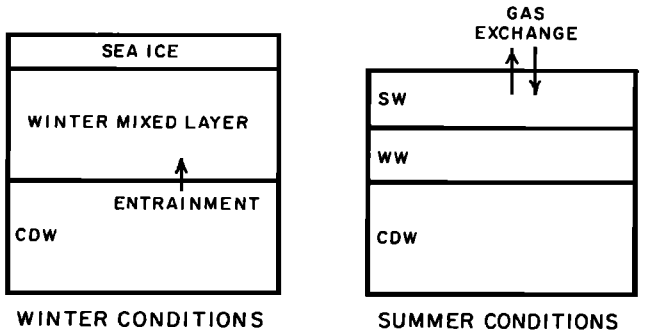


**Figure 12.** Sketch of the upper water layers for winter and summer conditions (for explanation, see text).

layer, $^{14}C$ exchange rate, period of time during which gas exchange with the atmosphere is suppressed by ice cover) mask the error in the determination of the prebomb value of CDW. During summer, a surface layer of about 55 m thickness is allowed to exchange with the atmosphere for a period of 6 months (Figure 12). Before the next winter period with its related entrainment of "old" CDW, the upper water column consisting of surface water is mixed with the remnant of the winter mixed layer (unchanged in our model during summer). The reconstruction of the atmospheric $^{14}C$ concentrations as a function of time is described by *Schlosser et al.* [1989]. The model is run from 1900 to 1987 to achieve equilibrium conditions for the prebomb era.

The simulated $\Delta^{14}C$ values for SW and WW are tuned to the available measurements from 1972 (GEOSECS station 89 [*Östlund et al.*, 1987]), 1973 (IWSOE [*Weiss et al.* 1979]), 1985 (ANT III [*Schlosser et al.* 1987]), 1986 (ANT V/2/3), and 1987 (ANT V/4) (Figure 13). The simulated $\Delta^{14}C$ values of WW are lower than those of SW (about 10 to 70 ‰). This feature is generally consistent with the available measurements. However, it does not hold true for the ANT V/2 data from the winter mixed layer and for the ISWOE data. The ANT V/2 data are winter data collected on a north/south section into the ice and therefore cover the range from more or less pure surface water to a fully developed winter mixed layer (pure WW). There is no obvious explanation for the deviation of the IWSOE data from the simulated line. The most likely reason for the difference seems to be natural variability of the surface layer dynamics. Such variability is obvious from the observation of the Weddell Sea polynya in the late 1970s.

The $^{14}C$ simulations yield prebomb $\Delta^{14}C$ values of about −132 ‰ for SW and −145 ‰ for WW. We estimate the uncertainty of these values to be of the order of ±5 to 10 ‰ based on variations of the individual parameters used in our simple model. The estimated prebomb $\Delta^{14}C$ value of surface water is in close agreement with the value of about −125 ‰ at 60°S estimated by *Bard* (1988) who used a synthesis of prebomb surface $^{14}C$ measurements and the *Broecker et al.* [1985] prebomb $^{14}C$ levels derived from the comparison of GEOSECS tritium and $^{14}C$ profiles.

**Deep Water** The deep water with temperatures around 0 °C ($^{14}C$ minimum) contains only a small bomb $^{14}C$ component. This is evident from (1) the comparison of the $\Delta^{14}C$ values of this water with those of lower CDW in Drake Passage (GEOSECS data and unpublished data from WOCE WHP line S 1 obtained in early 1990), (2) the low tritium concentrations found in these waters [*Bayer and Schlosser*, 1991], and (3) the comparison with data obtained in the northern Weddell Sea during GEOSECS (station 89). We therefore believe that for a first-order estimate of the WSDW prebomb $\Delta^{14}C$ values we can use the tritium/$^{14}C$ ratio of the

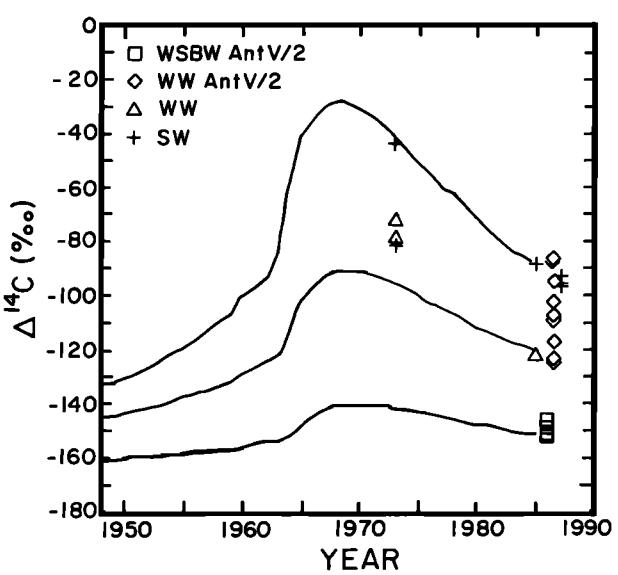


**Figure 13.** Simulation of $\Delta^{14}C$ as a function of time for surface water (SW) and winter water (WW); for explanation, see text.

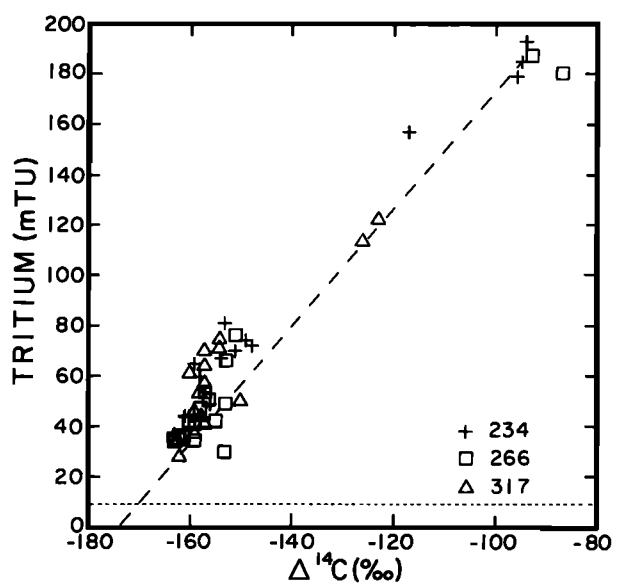


**Figure 14.** Tritium versus $\Delta^{14}C$ plot for three stations from the 0° longitude section. The short-dashed line at 10 mTU indicates the best guess for the prebomb tritium level of the deep waters in the Weddell Sea.

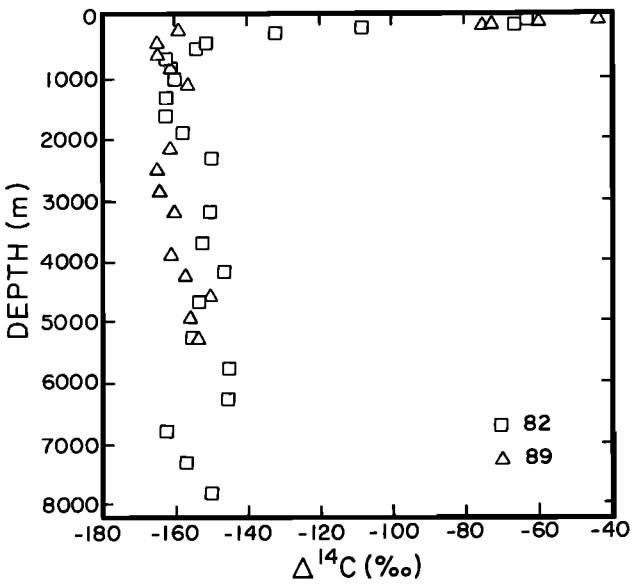


**Figure 15.** $\Delta\,^{14}C$ versus depth profiles for two GEOSECS stations located in the Weddell Sea.

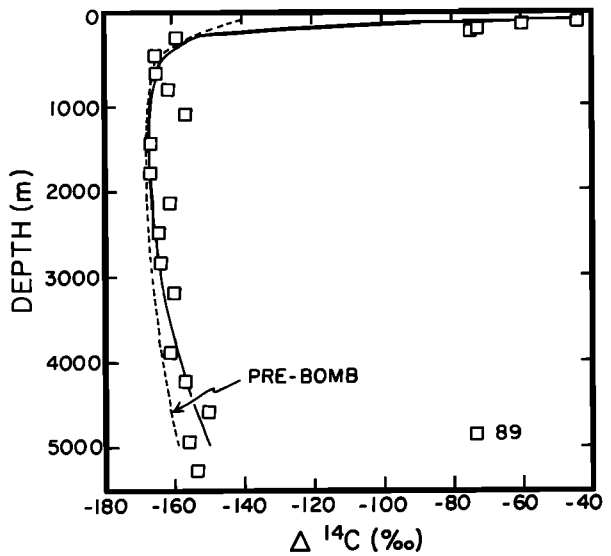


**Figure 16.** Reconstruction of the prebomb Weddell Sea $\Delta\,^{14}C$ profile together with the $\Delta\,^{14}C$ profile of GEOSECS station 89.

waters from depths around the 0 °C isotherm for subtraction of the bomb $^{14}C$ component by extrapolating the tritium/$^{14}C$ ratio to the estimated prebomb tritium value. If we assume that the prebomb tritium concentration of WSDW was zero, we obtain a prebomb $\Delta\,^{14}C$ of about −174 ‰ (Figure 14). If we set the prebomb tritium concentration to 10 mTU (best guess), the prebomb $\Delta\,^{14}C$ is estimated to be −170 ‰, only slightly different from the value for zero prebomb tritium.

Our estimate is consistent with the measurements obtained from GEOSECS station 89 sampled in 1972 [*Stuiver and Östlund*, 1980]. Minimum $\Delta\,^{14}C$ values at this stations are about −167 ‰ at about 1500-m depth (Figure 15), i.e., close to those observed at WWSP station 234, which has approximately the same geographical position (Plate 2). Considering a small bomb $^{14}C$ component which is more difficult to subtract than for the 1986 data due to the missing sensitivity of the GEOSECS tritium measurements (tritium concentrations are practically zero below several hundred meters on the basis of a detection limit of 0.05 TU), we conclude that the prebomb $^{14}C$ of WSDW (0 °C) did not significantly change between 1972 and 1986.

**Bottom Water** If we assume that WSBW is a mixture of shelf water and CDW, we can use the prebomb $\Delta\,^{14}C$ estimated for these water masses together with their relative contributions to WSBW derived from temperature/salinity data to estimate the prebomb $\Delta\,^{14}C$ of WSBW. In this estimate we assume that the $\Delta\,^{14}C$ values of shelf water are close to those of SW and WW (we use an average value of −135 ‰). Setting the temperature of shelf water to −1.87 °C and that of WSBW to −0.7 °C, the ratio of CDW to shelf water is determined to be 63/37. The prebomb $^{14}C$ of WSBW can then be calculated to be −157 ‰ (0.63 times −170 ‰ + 0.37 times −135 ‰). The prebomb value of WSBW can also be determined as a function of time to estimate how strong the bomb $^{14}C$ signal influenced the $\Delta\,^{14}C$ of WSBW during the past 3 decades (Figure 13). It is evident that bomb $^{14}C$ caused a small but significant elevation of the $\Delta\,^{14}C$ value of WSBW.

## Bomb $^{14}C$ Water Column Inventories

As pointed out by *Broecker et al.* [1985], comparison of estimated bomb $^{14}C$ delivery to the ocean with measured water column bomb $^{14}C$ inventories provides constraints on the lateral transport in the ocean. We used our estimated prebomb $^{14}C$ values to reconstruct the rough shape of the natural $^{14}C$ profile in the Weddell Sea (Figures 16 and 17 ). Comparison of measured $^{14}C$ profiles during GEOSECS and WWSP 86 allows estimation of the bomb $^{14}C$ water column inventories in 1973 and 1986.

We estimate bomb $^{14}C$ water column inventories for

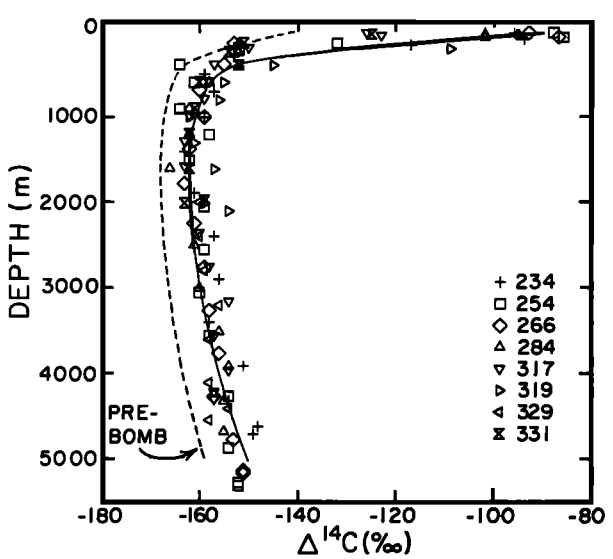


**Figure 17.** Same as Figure 16 for WWSP 86 stations.

the Atlantic south of 60°S of about $18.6 \times 10^{25}$ atoms (area is $5.3 \times 10^6$ km$^2$, *Broecker et al.* [1985]) for 1973 and of about $36.9 \times 10^{25}$ atoms for 1986. The value estimated for 1973 is significantly higher than that obtained by *Broecker et al.* [1985]. The most likely reasons for the discrepancy between the two estimates are (1) the lower surface $\Delta\,^{14}C$ value used in our calculation and (2) the fact that we added the small, but significant bomb $^{14}C$ component in the deep water to our inventory estimates.

## Conclusions

We consider our measurements as a first-order description of the $^{14}C$ and $^{39}Ar$ distributions in the Weddell Sea including the eastern and southern shelves and the continental slope north of Filchner Depression. They are consistent with the hydrography and circulation of the Weddell Sea as far as they are presently known. The data can be used for first-order estimates of the prebomb $^{14}C$ of Weddell Sea surface and deep waters. These estimates are consistent with the few prebomb $^{14}C$ measurements in Antarctic waters. Our estimates can probably be improved once a more complete data set including the northwestern shelves and models for simulation of transient tracers in the main water masses becomes available. Our data provide a reliable estimate of the initial $^{39}Ar$ concentration of Weddell Sea Bottom Water and Antarctic Bottom Water. These values are important for the evaluation of the global oceanic $^{39}Ar$ distribution.

**Acknowledgments.** This study profited from the support of numerous collegues and institutions: H.G. Junghans extracted the $CO_2$ from the large-volume water samples and solved critical problems of our equipment at sea. W. Roether, M. Rhein, F. Zaucker, G. Bader, and H. Werner helped to collect the large-volume samples during legs 2 and 3 of ANT V. Peter Kalt was responsible for the collection of $^{39}Ar$ samples during ANT V/2. The salinity and nutrient measurements used for quality control of the large-volume samples were provided by the Ocean Data Facility of the Scripps Institution of Oceanography. The Alfred-Wegener-Institute for Polar and Marine Research provided logistical support for the *Polarstern* cruises. Officers and crew of RV *Polarstern* guaranteed a successful field program by their steady support at sea. Financial support was provided by the Deutsche Forschungsgemeinschaft, the Schweizer Nationalfond, and the National Science Foundation (grant DPP 90-25099). L-DEO contribution no. 5185.

## References

Bard, E., Correction of accelerator mass spectrometry $^{14}C$ ages measured in planktonik foraminifera: Paleoceanographic implications, *Paleoceanography, 3*, 635–645, 1988.

Bayer, R., and P. Schlosser, Tritium profiles in the Weddell Sea, *Mar. Chem., 35*, 123–136, 1991.

Broecker, W.S., R. Gerard, M. Ewing, and B.C. Heezen, Natural radiocarbon in the Atlantic Ocean, *J. Geophys. Res., 65*, 2903–2931, 1960.

Broecker, W.S., T.H. Peng, G. Östlund, and M. Stuiver, The distribution of bomb radiocarbon in the ocean, *J. Geophys. Res., 90*, 6953–6970, 1985.

Broecker, W.S., S. Blanton, W.M. Smethie, and G. Östlund, Radiocarbon decay and oxygen utilization in the deep Atlantic Ocean, *Global Bio. Geochem. Cycles, 5*, 87–117, 1991.

Carmack, E.C., and T.D. Foster, On the flow of water out of the Weddell Sea, *Deep Sea Res., 22*, 711–725, 1975a.

Carmack, E.C., and T.D. Foster, Circulation and distribution of oceanographic properties near the Filchner Ice Shelf, *Deep Sea Res., 22*, 77–90, 1975b.

Foldvik, A., and T. Gammelsrød, Notes on Southern Ocean hydrography, sea-ice and bottom water formation, *Paleoceanogr. Paleoclimatol. Paleoecol., 67*, 3–17, 1988.

Foldvik, A., T. Gammelsrød, and T. Tørresen, Circulation and water masses on the southern Weddell Sea shelf, in *Oceanology of the Antarctic Continental Shelf, Antarct. Res. Ser.*, vol. 43, edited by S.S. Jacobs, pp. 5–20, AGU, Washington, D.C., 1985a.

Foldvik, A., T. Gammelsrød, and T. Tørresen, Hydrographic observations from the Weddell Sea during the Norwegian Antarctic Research Expedition 1976/1977, *Polar Res., 3*, 177–193, 1985b.

Foldvik, A., T. Gammelsrød, and T. Tørresen, Physical oceanography studies in the Weddell Sea during the Norwegian Antarctic Research Expedition 1978/79, *Polar Res., 3*, 195–207, 1985c.

Foster, T.D., and E.C. Carmack, Frontal zone mixing and Antarctic Bottom Water formation in the southern Weddell Sea, *Deep Sea Res., 26*, 741–762, 1976.

Gordon, A.L., and B.A. Huber, Thermohaline stratification below the Southern Ocean sea ice, *J. Geophys. Res., 89*, 641–648, 1984.

Gordon, A.L., and B.A. Huber, Southern Ocean winter mixed layer, *J. Geophys. Res., 95*, 11,655–11,672, 1990.

Kromer, B., Recalibration of Heidelberg $^{14}C$ laboratory data, *Radiocarbon, 26*, 148, 1984.

Kromer, B., C. Pfleiderer, P. Schlosser, I. Levin, K.O. Münnich, G. Bonani, M. Suter, and W. Wölfli, AMS $^{14}C$ measurement of small volume oceanic water samples: Experimental procedure and comparison with low-level counting technique, *Nucl. Instrum. Methods*, B*29*, 302–305, 1987.

Loosli, H.H., A dating method with $^{39}Ar$, *Earth Planet. Sci. Lett., 63*, 51–62, 1983.

Münnich, K.O., and W. Roether, Transfer of bomb $^{14}C$ and tritium from the atmosphere to the ocean; internal mixing of the ocean on the basis of tritium and $^{14}C$ profiles, Symposium on Radioactive Dating and Methods of Low-Level Counting, *Rep. UN DOC SM-87/22*, pp. 93–103, Int. At. Energy Agency, Vienna, 1967.

Östlund, H.G., H. Craig, W.S. Broecker, and D. Spencer, GEOSECS Atlantic, Pacific, and Indian Ocean Expeditions, volume 7, shorebased data and graphics. National Science Foundation, Washington, D.C., 1987.

Schlitzer, R., W. Roether, U. Weidmann, H.H. Loosli and P. Kalt, A meridional $^{14}C$ and $^{39}Ar$ section in the northeast Atlantic deep water, *J. Geophys. Res., 90*, 6945–6952, 1985

Schlosser, P., C. Pfleiderer, B. Kromer, I. Levin, K.O. Münnich, G. Bonani, M. Suter, and W. Wölfli, Measurement of small volume oceanic $^{14}C$ samples by accelerator mass spectrometry, *Radiocarbon, 29*, 347–352, 1987.

Schlosser, P., B. Kromer, K.O. Münnich, and R. Bayer, $^{14}C$ profiles in the central Weddell Sea, *Radiocarbon, 31*, 544–556, 1989.

Schlosser, P., R. Bayer, A. Foldvik, T. Gammelsrød, G. Rohardt, and K.O. Münnich, Oxygen 18 and helium as trac-

ers of Ice Shelf Water and water/ice interaction in the Weddell Sea, *J. Geophys. Res.*, *95*, 3253–3263, 1990.

Schlosser, P., J.L. Bullister, and R. Bayer, Studies of deep water formation and circulation in the Weddell Sea using natural and anthropogenic tracers, *Mar. Chem.*, *35*, 97–122, 1991.

Sievers, H.A., and W.D. Nowlin Jr., The stratification and water masses at Drake Passage, *J. Geophys. Res.*, *89*, 10489–10514, 1984.

Stuiver, M., and H.G. Östlund, GEOSECS Atlantic radiocarbon, *Radiocarbon*, *25*, 1–29, 1980.

Stuiver, M., and H.A. Polach, Reporting of $^{14}C$ data, *Radiocarbon*, *19*, 355–363, 1977.

Stuiver, M., P. Quay, and G. Östlund, Abyssal water carbon-14 distribution and the age of the worlds oceans, *Science*, *219*, 849–851, 1983.

Weiss, R.F., H.G. Östlund, and H. Craig, Geochemical studies of the Weddell Sea, *Deep Sea Res.*, *26*, 1093–1120, 1979.

Whitworth, T., III, and W.D. Nowlin Jr., Water masses and currents of the Southern Ocean at the Greenwich Meridian, *J. Geophys. Res.*, *92*, 6462–6476, 1987.

---

R. Bayer and B. Kromer, Institut für Umweltphysik der Universität Heidelberg, Im Neuenheimer Feld 366, D-69 Heidelberg, Germany.

G. Bonani and M. Suter, Institut für Mittelenergiephysik, ETH Zürich, Hönggerberg, CH-8093, Zürich, Switzerland.

H. H. Loosli, Physikalisches Institut der Universität Bern, Sidlerstr. 5, CH-3012 Bern, Switzerland.

P. Schlosser and R. Weppernig, Lamont–Doherty Earth Observatory, Palisades, N.Y. 10964.

(Received March 29, 1993; revised November 8, 1993; accepted December 27, 1993.)